

Real-time process dynamics monitoring in Anammox reactors

B. Alpaslan Kocamemi and D. Dityapak

ABSTRACT

Process dynamics in Anammox systems were evaluated through continuous monitoring of pH, oxidation reduction potential (ORP) and conductivity in two separate newly started-up sequencing batch reactors, one seeded with an enriched Anammox sludge and the other seeded with mixed activated sludge. The pH and ORP profiles exhibited characteristic patterns depending on the process dynamics during early start-up, start-up and enrichment phases of the operational period of 410 days. The simultaneously continuing processes of the start-up period showed apparent indicative trend lines in pH and ORP profiles. Conductivity profiles were consistent with the process dynamics in all phases. During the enrichment phase, conductivity decreases could quantitatively be related to process removal efficiencies and all real-time profiles exhibited specific break-points which coincided with the end of Anammox in each cycle. The end of Anammox was observed as an 'apex' on pH profiles and a 'valley' on ORP profiles. The 'apex' and 'valley' points exactly coincided with the end point of the linear decrease in the conductivity profiles. The overall findings suggested a great potential in using real-time pH, ORP and conductivity measurements for quick and reliable monitoring of Anammox systems during start-up and enrichment periods.

Key words | Anammox, conductivity, enrichment, ORP, pH, start-up

B. Alpaslan Kocamemi (corresponding author)
D. Dityapak
Marmara University,
Faculty of Engineering,
Environmental Engineering Department,
Istanbul,
Turkey
E-mail: bilge.alpaslan@marmara.edu.tr

INTRODUCTION

The Anammox process, which was discovered by [Mulder *et al.* \(1995\)](#), is a chemolithoautotrophic biological process converting $\text{NH}_4^+\text{-N}$ directly into N_2 gas under anaerobic conditions using $\text{NO}_2^-\text{-N}$ as the electron acceptor by a group of Planctomycete bacteria ([Van Loodsrecht & Salem 2006](#)).

The first full-scale Anammox reactor went into operation in 2002 in a sludge treatment plant in Rotterdam, The Netherlands ([Van Der Star *et al.* 2007](#)). Since then, the number of reported full-scale Anammox installations has been very limited. The main challenge to a full-scale implementation of the Anammox process in wastewater treatment is its long and difficult start-up period, which is directly dependent on reactor configuration, seeding strategy, monitoring and control of process dynamics. The sequencing batch reactor (SBR) is a widely accepted reactor configuration for Anammox enrichment due to its simplicity and its efficiency for biomass retention ([Strous *et al.* 1998](#)). With regard to seeding strategy, studies for the evaluation of the use of local mixed activated sludge samples as inocula to start up a new Anammox system have been widely

performed ([Bae *et al.* 2010](#); [Sun *et al.* 2011](#)). Another strategy for quick and efficient management of a newly started-up Anammox reactor may be the use of real-time measurements of the main operational parameters (e.g., oxidation reduction potential (ORP) and pH), which has been proven successful for the monitoring of nitrification and denitrification processes ([Akin & Ugurlu 2005](#)). Unfortunately, no more than a few studies ([Szatkowska *et al.* 2005](#); [Lackner & Horn 2012](#); [Li *et al.* 2012](#)) evaluating the process dynamics of Anammox reactors via real-time measurements have been performed until now. In the study of [Szatkowska *et al.* \(2005\)](#), conductivity profiles in a partial nitrification–Anammox system were parallel to the plots of nitrogen forms. Thus, it was concluded that conductivity could be implemented as an Anammox monitoring tool. [Lackner & Horn \(2012\)](#) demonstrated that ORP could be used as a monitoring parameter for detection of $\text{NH}_4^+\text{-N}$ depletion in a nitrification–Anammox system. In the study of [Li *et al.* \(2012\)](#), pH and conductivity measurements were related to process performance in an Anammox reactor. To the best

of our knowledge, there has been no study for the evaluation of pH, ORP, conductivity profiles together for an Anammox system and their correlation with process performance. Therefore, further research is necessary to investigate the feasibility of using real-time pH, ORP and conductivity measurements to follow process dynamics in Anammox reactors, especially for the start-up and enrichment periods.

In this study, the start-up and enrichment periods of two different SBR systems, one (SBR1) inoculated with enriched Anammox seed and the other (SBR2) inoculated with a mixed activated sludge seed, were continuously monitored via real-time pH, ORP and conductivity measurements during a 410-day operation period. The measurement profiles were evaluated based on observed nitrogen removal efficiencies in the systems. The overall objective was to investigate the potential of using real-time pH, ORP and conductivity measurements to monitor process dynamics in Anammox systems during the start-up and enrichment periods. The use of two different types of inocula also enabled us to evaluate how microbial diversity in seed sludge affects the follow-up process dynamics via real-time on-line measurements.

MATERIALS AND METHODS

Two plexi-glass SBRs (Figure 1), each with a working volume of 4.5 L, were inoculated with the enriched Anammox sludge seed from the first worldwide Anammox system treating up to 750 kg N/d in Rotterdam, The Netherlands (Van Der Star *et al.* 2007) (SBR1), and the mixed activated sludge seed from a local sewage treatment plant in Istanbul, Turkey (SBR2), respectively. The initial biomass concentration in both reactors was around 3,000 mg volatile suspended solids (VSS)/L.

The reactors were operated continuously for 410 days by feeding with stock synthetic wastewater composed of the following: 5–1,166 mg/l $\text{NH}_4^+\text{-N}$, 5–1,400 mg/l $\text{NO}_2^-\text{-N}$, 25–30 mg/l $\text{NO}_3^-\text{-N}$ and 525–1,250 mg/l KHCO_3 for SBR1; 75–750 mg/l $\text{NH}_4^+\text{-N}$, 75–975 mg/l $\text{NO}_2^-\text{-N}$, 50 mg/l $\text{NO}_3^-\text{-N}$ and 1,000–1,250 mg/l KHCO_3 for SBR2; 27.2 mg/l K_2HPO_4 , 300 mg/l $\text{MgSO}_4 \cdot 7\text{H}_2\text{O}$ and 180 mg/l $\text{CaCl}_2 \cdot 2\text{H}_2\text{O}$ for both SBR1 and SBR2. To each litre of the reactors, 1 ml of trace element solution I including 5 g/l $\text{Na}_2\text{EDTA} \cdot 2\text{H}_2\text{O}$ and 5 g/l $\text{FeSO}_4 \cdot 7\text{H}_2\text{O}$ and 1 ml of trace element solution II including 15 g/l $\text{Na}_2\text{EDTA} \cdot 2\text{H}_2\text{O}$, 0.43 g/l $\text{ZnSO}_4 \cdot 7\text{H}_2\text{O}$,

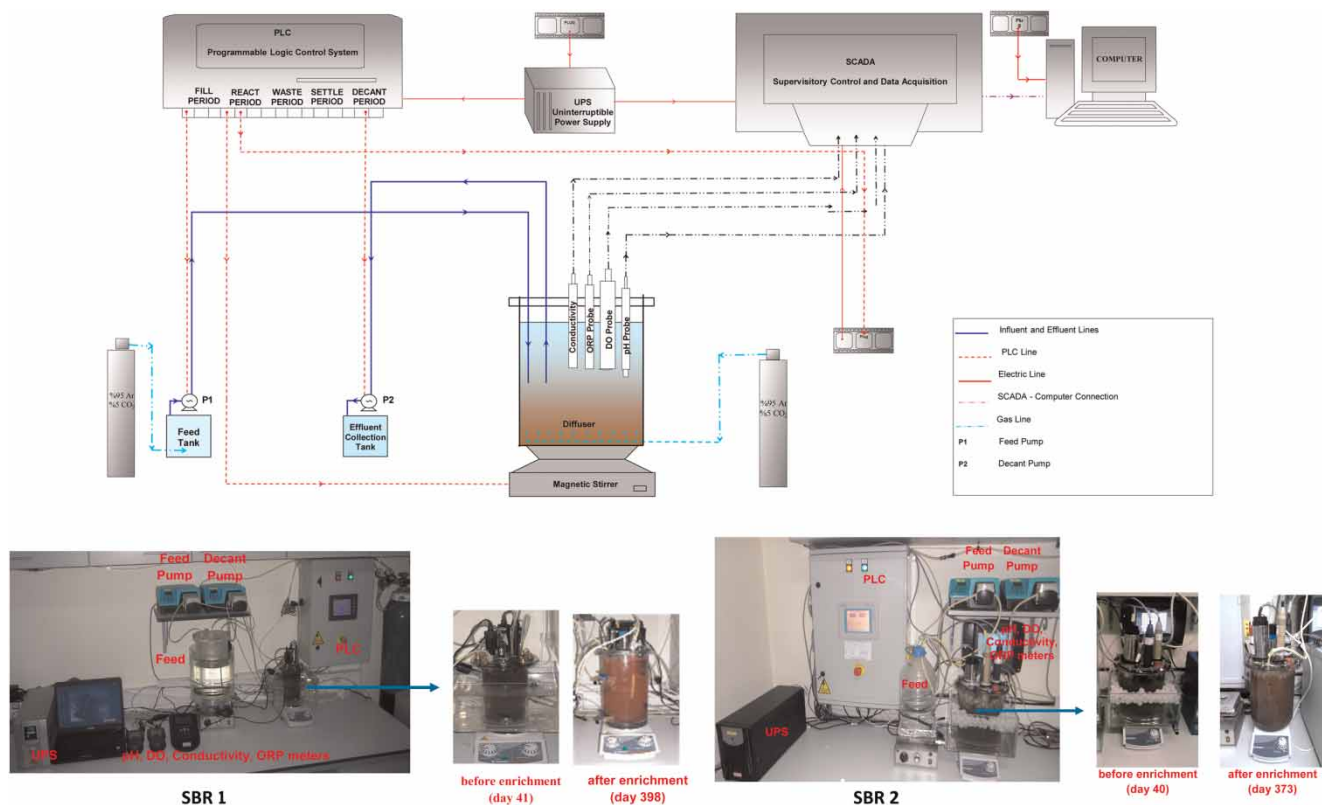


Figure 1 | A schematic operation diagram and set-up photos of the SBR systems.

0.011 g/l H_3BO_3 , 0.25 g/l $\text{CuSO}_4 \cdot 5\text{H}_2\text{O}$, 0.99 g/l $\text{MnCl}_2 \cdot 4\text{H}_2\text{O}$, 0.12 g/l CoCl_2 , 0.19 g/l $\text{NiCl}_2 \cdot 6\text{H}_2\text{O}$, and 0.10 g/l Na_2SeO_3 were added. The $\text{NH}_4^+\text{-N}$ and $\text{NO}_2^-\text{-N}$ loadings to the reactors were increased stepwise (Figure 2) depending on the treatment efficiencies. $\text{NO}_3^-\text{-N}$ was fed continuously to the reactors for the consumption of organic matter possibly generated from endogenous decay activity during early stages of start-up.

The operational cycles of the reactors, including fill, react, settle and decant phases, were kept around 24 h using programmable logic controller (PLC) systems (Siemens CPU 224). Hydraulic retention time (HRT) was held around 4.5 days with an influent flow-rate of 1 L/d. In order to maintain anaerobic conditions and to supply inorganic C, liquid and gas phases of the reactors were continuously

flushed with a 95% Ar -5% CO_2 gas mixture introduced from pressurized gas cylinders with proper regulator systems. They were operated at a fixed temperature of around 34°C using thermostated water jackets. Magnetic stirrers were used to achieve complete mixing conditions.

The pH, ORP, conductivity and dissolved oxygen (DO) parameters were continuously measured by periodically calibrated on-line Hach-Lange probes in both reactors and recorded at 15-minute time intervals. DO levels were monitored around 0 ± 0.07 mg/l.

Duplicate samples withdrawn daily from the feed (Figure 1) and effluent tanks collecting reactor decants at the end of daily batch cycles (Figure 1) were analyzed for $\text{NH}_4^+\text{-N}$, $\text{NO}_2^-\text{-N}$ and $\text{NO}_3^-\text{-N}$ after filtering through 0.45 μm Millipore filters. These

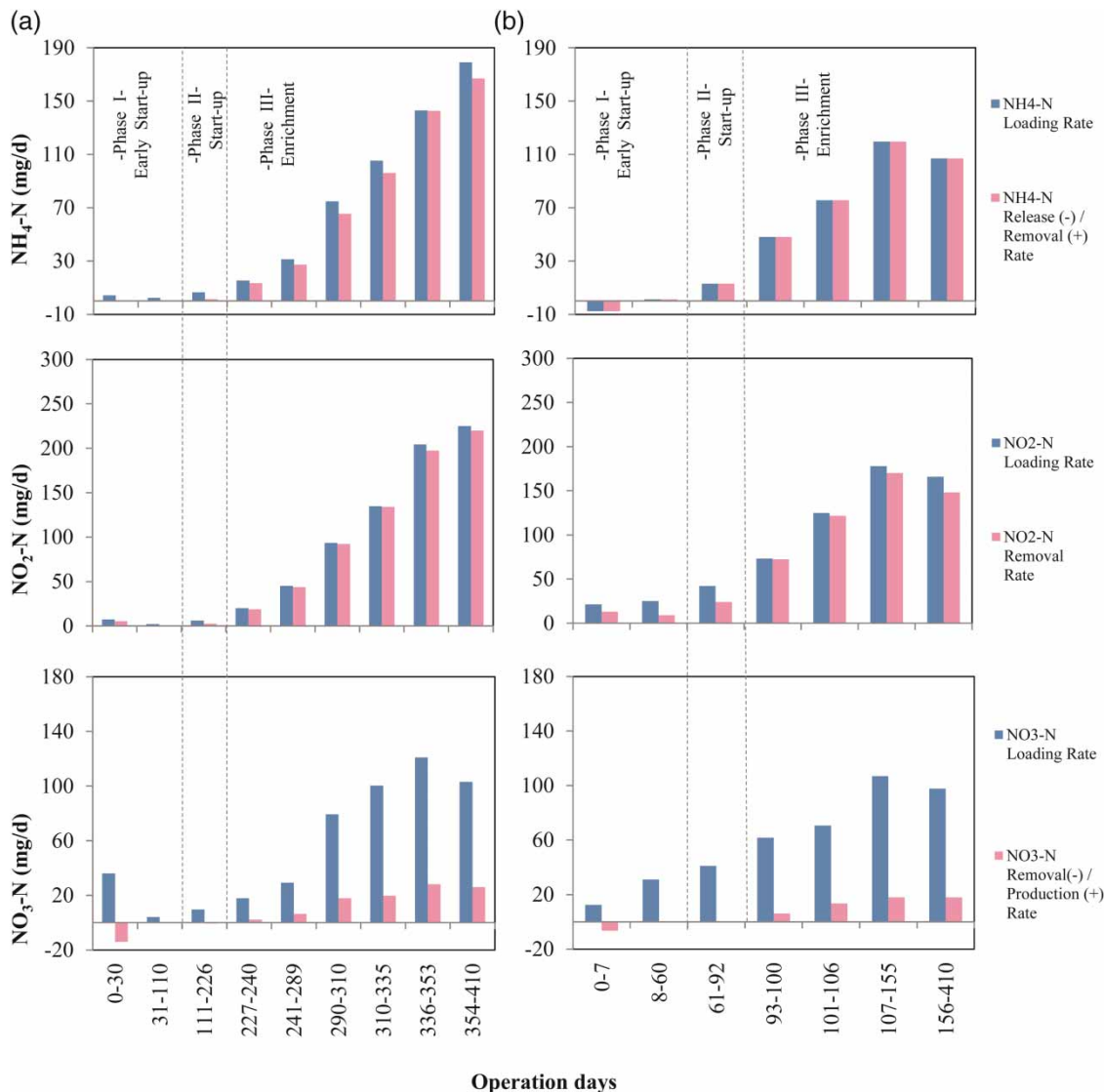


Figure 2 | Process dynamics through 410-day start-up and enrichment period for (a) SBR1 and (b) SBR2.

analyses were performed via a Shimadzu Prominence HIC-SP-dual injection ion chromatograph equipped with Shimpack IC-SC1 cation column and Shimpack IC-SA2 anion column, using 3.5 mM H₂SO₄ mobile phase and 12 mM NaHCO₃-0.6 mM Na₂CO₃ mobile phase, respectively.

VSS measurements were conducted according to *Standard Methods* (1998).

Fluorescence in situ hybridization (FISH) analyses of sludge samples were performed using 16S rRNA targeting oligonucleotide probes Planc 040, Amx 368, Amx 820, Bs 820, Kst1275 (Schmid *et al.* 2005).

RESULTS AND DISCUSSION

The process dynamics in both reactors exhibited similar patterns with different durations despite markedly different inocula. The 410-day operational period was divided into three main phases (Figure 2): (I) early start-up, (II) start-up and (III) enrichment. The overall real-time pH, ORP and conductivity data collected through these phases are shown in Figure 3. Both Figures 2 and 3 have to be evaluated together in order to see the reflection of the loading and treatment performance changes of the reactors and operational problems

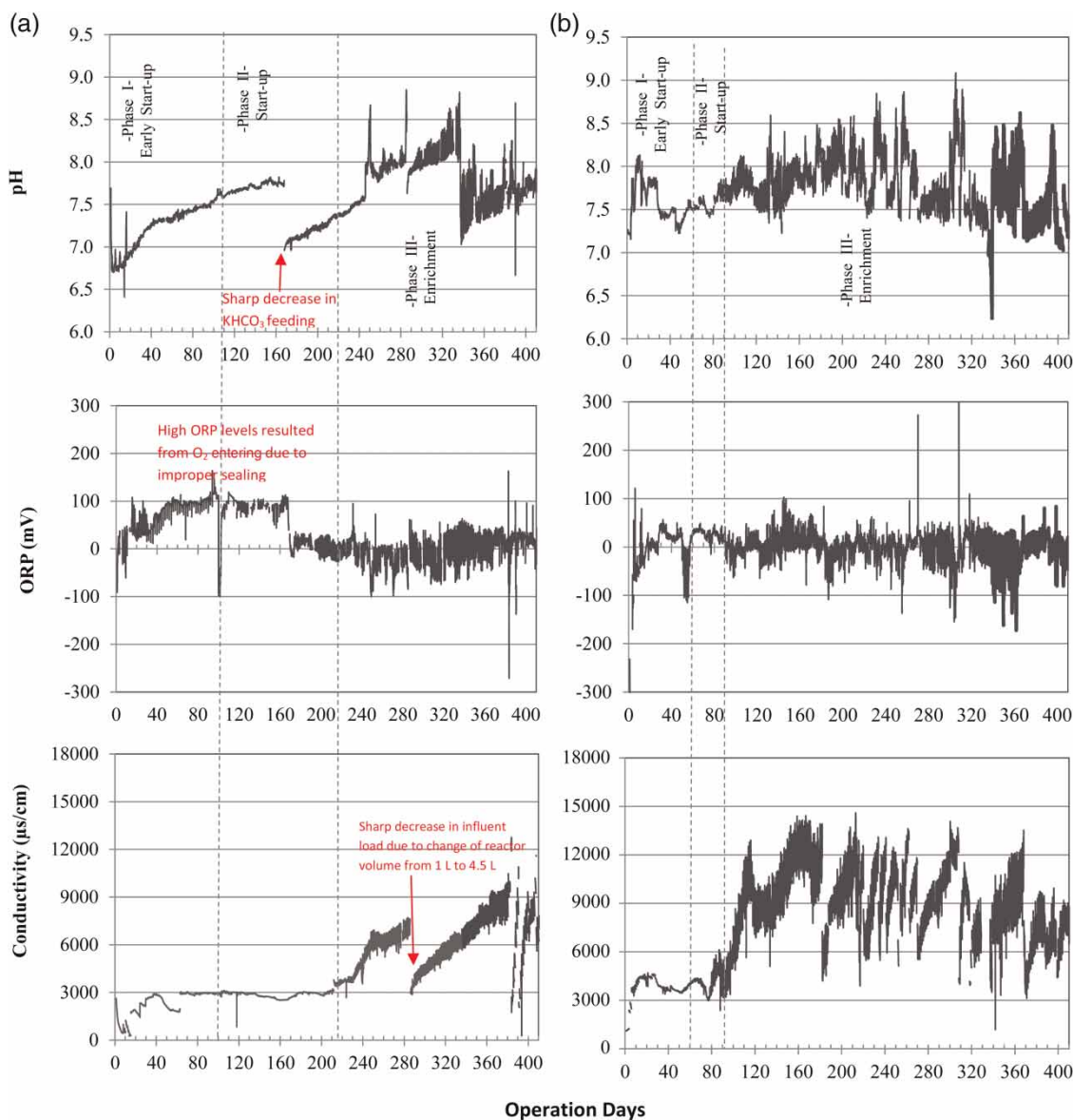


Figure 3 | Real-time pH, ORP and conductivity measurements through the 410-day start-up and enrichment period for (a) SBR1 and (b) SBR2.

on real-time measurement profiles over the entire experimental period. Sample graphs showing pH, ORP and conductivity changes through a daily batch cycle in each phase are given in Figure 4 for SBR1 and Figure 5 for SBR2.

In the early stages of start-up (Phase I), a slight increase in $\text{NH}_4^+\text{-N}$ and significant decrease in $\text{NO}_2^-\text{-N}$ and $\text{NO}_3^-\text{-N}$ levels were clearly observed (Figure 2) for both reactors, indicating that endogenous denitrification due to the decay of seed sludge predominated. In batch cycles (Figures 4(a) and 5(a)), pH exhibited an increasing trend as expected from denitrification producing alkalinity (Table 1). In SBR1, ORP values were always positive and ranged between +20 and +40 mV without any drop due to $\text{NO}_2^-\text{-N}$ and $\text{NO}_3^-\text{-N}$ depletion through denitrification. This mainly resulted from atmospheric O_2 entering the reactor because of improper sealing. As opposed to SBR1, batch cycles started with ORP around -80 mV in properly sealed SBR2. ORP rapidly increased from -80 mV to -40 mV with feeding. Both ORP and conductivity decreased gradually with depletion of $\text{NO}_2^-\text{-N}$ and

$\text{NO}_3^-\text{-N}$ via endogenous denitrification through the cycle. However, the decreasing rate of conductivity in SBR2 was approximately tenfold greater than that of SBR1. This might be strongly related to the seed origin of SBR2. Being seeded with mixed activated sludge, endogenous decay activity was more intense in SBR2 relative to SBR1, which was seeded with enriched Anammox sludge (Figure 2). Linearly decreasing conductivity profiles were further evaluated to find a quantitative correlation between observed conductivity decreases and changes in nitrogen species. Using average influent and effluent $\text{NO}_2^-\text{-N}$ and $\text{NO}_3^-\text{-N}$ (Figures 4(a) and 5(a)), the expected stoichiometric conductivity decreases through endogenous denitrification either via $\text{NO}_2^-\text{-N}$ or $\text{NO}_3^-\text{-N}$ routes were calculated based on Table 1. For both reactors, the calculated conductivity decreases (around $20 \mu\text{S}/\text{cm}$ for SBR1, $30 \mu\text{S}/\text{cm}$ for SBR2) did not match the observed ones (around $50 \mu\text{S}/\text{cm}$ for SBR1 (Figure 4(a)), $500 \mu\text{S}/\text{cm}$ for SBR2 (Figure 5(a))). For SBR2, the reason for the large gap between observed and calculated conductivity decreases was most probably

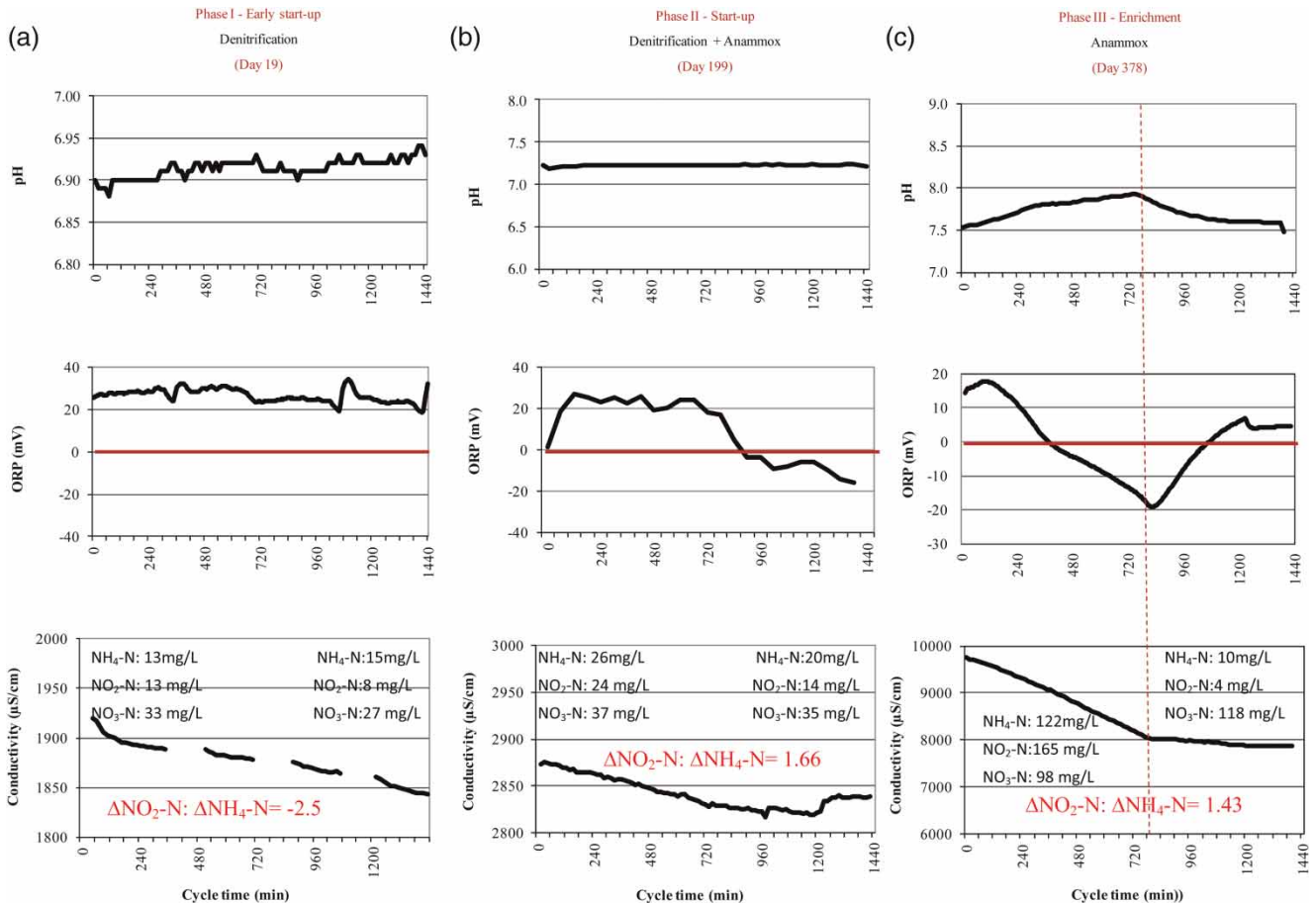


Figure 4 | Sample real-time pH, ORP and conductivity measurements observed in batch cycles of SBR1 during (a) Phase I, (b) Phase II and (c) Phase III.

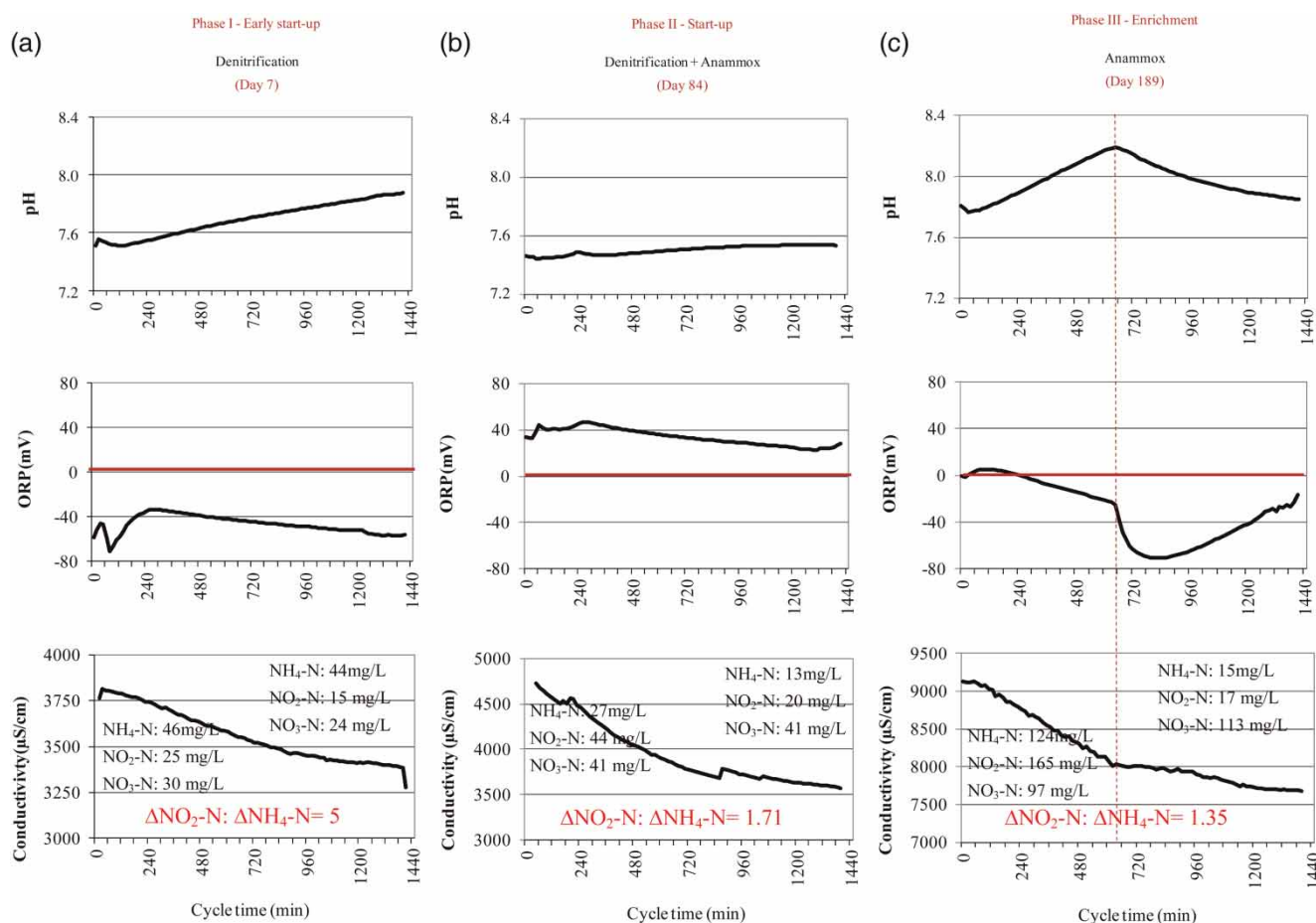


Figure 5 | Sample real-time pH, ORP and conductivity measurements observed in batch cycles of SBR2 during (a) Phase I, (b) Phase II and (c) Phase III.

due to other processes continuing simultaneously with the dominant endogenous denitrification activity.

In Phase II of the reactors (Figure 2), slight decreases were observed in $\text{NH}_4^+\text{-N}$ with simultaneous decreases in $\text{NO}_2^-\text{-N}$ indicating the start of the Anammox process. However, there was still $\text{NO}_3^-\text{-N}$ decrease in both reactors. Moreover, the decreases observed in $\text{NH}_4^+\text{-N}$ and $\text{NO}_2^-\text{-N}$ did not match with Anammox stoichiometry. These observations indicated that endogenous denitrification and Anammox were processes that continued simultaneously. Consistent with the process dynamics, the pH profile of SBR2 (Figure 5(b)) exhibited an increasing trend mainly due to alkalinity produced from denitrification and slightly due to acidity consumption through the newly started Anammox process (Table 1). However, in SBR1, the pH profile was almost straight. This might be related to the continuous CO_2 purging of the reactors to supply inorganic C. The generation of alkalinity with endogenous denitrification activity somehow balanced the pH drop due to CO_2 purging. At the start of each batch cycle, the initial ORP was positive

in both reactors due to $\text{NO}_2^-\text{-N}$ and $\text{NO}_3^-\text{-N}$ remaining from the previous cycle. ORP increase was observed during feeding. This increase was slighter in SBR2 since it was fed with a high concentration of the reduced compound $\text{NH}_4^+\text{-N}$ relative to SBR1 (Figure 2). ORP profiles of both reactors exhibited a plateau with different durations after feeding. The wider plateau of SBR1 might have resulted from resistance created through the $\text{NH}_4^+\text{-N}$, $\text{NO}_2^-\text{-N}$ and $\text{NO}_3^-\text{-N}$ removal dynamics that continued simultaneously in that period. $\text{NO}_3^-\text{-N}$ production via Anammox was not detectable in that period. However, $\text{NO}_3^-\text{-N}$ might have been produced via Anammox and then depleted suddenly through ongoing denitrification in the system. Hence, the removal of $\text{NO}_2^-\text{-N}$ and the $\text{NO}_3^-\text{-N}$ enhancing ORP drop were almost in balance with $\text{NH}_4^+\text{-N}$ removal and the most probable production of $\text{NO}_3^-\text{-N}$ enhancing the ORP increase. The plateau observed in the ORP profiles was followed by a gradual decrease as $\text{NO}_2^-\text{-N}$ and $\text{NO}_3^-\text{-N}$ were largely depleting due to denitrification. Conductivity values (Figures 4(b) and 5(b)) decreased gradually due to $\text{NO}_2^-\text{-N}$

Table 1 | Expected conductivity decreases in Anammox and denitrification processes based on molar conductivity per concentration values of the ions

Reaction		Change in ion content	mSm ² /mol N
Anammox process	$\text{NH}_4^+ + 1.32 \text{NO}_2^- + 0.066 \text{HCO}_3^- + 0.13 \text{H}^+ \rightarrow$ $1.02 \text{N}_2 + 0.26 \text{NO}_3^- + 0.066 \text{CH}_2\text{O}_{0.5}\text{N}_{0.15} + 2.03 \text{H}_2\text{O}$	- 1 NH ₄ ⁺	- 7.34
		- 1.32 NO ₂ ⁻	- 9.47
		- 0.066 HCO ₃ ⁻	- 0.29
		- 0.13 H ⁺	- 4.55
		+ 0.26 NO ₃ ⁻	+ 1.85
The expected conductivity decrease for 1 mole of NH₄-N removal or 1.32 mole NO₂-N removal			- 19.80
Denitrification process (via nitrate route)	$0.926 \text{NO}_3^- + \text{CH}_3\text{OH} + 0.22 \text{H}_2\text{CO}_3 \rightarrow$ $0.051 \text{C}_5\text{H}_7\text{O}_2\text{N} + 0.435 \text{N}_2 + 0.926 \text{HCO}_3^- + 1.56 \text{H}_2\text{O}$	- 0.926 NO ₃ ⁻	- 6.61
		+ 0.926 HCO ₃ ⁻	+ 4.12
The expected conductivity decrease for 0.926 mole of NO₃-N denitrification			- 2.49
Denitrification process (via nitrite route)	$1.49 \text{NO}_2^- + \text{CH}_3\text{OH} + 0.79 \text{H}_2\text{CO}_3 \rightarrow$ $0.059 \text{C}_5\text{H}_7\text{O}_2\text{N} + 0.72 \text{N}_2 + 1.49 \text{HCO}_3^- + 1.84 \text{H}_2\text{O}$	- 1.49 NO ₂ ⁻	- 10.70
		+ 1.49 HCO ₃ ⁻	+ 6.63
The expected conductivity decrease for 1.49 mole of NO₂-N denitrification			- 4.07

NH₄⁺ = 7.34 mSm²/mol, NO₂⁻ = 7.18 mSm²/mol, HCO₃⁻ = 4.45 mSm²/mol, H⁺ = 35 mSm²/mol, NO₃⁻ = 7.14 mSm²/mol (CRC 1999).

and NO₃⁻-N depletion via denitrification and NH₄⁺-N and NO₂⁻-N depletion through Anammox. The NO₃⁻-N produced at undetectable levels in the newly started Anammox had negligible effect on conductivity decreases. The decreasing rate of conductivity in SBR2 was almost twofold greater than the one in SBR1. Consistently, observed process dynamics (Figure 2) indicated higher NH₄⁺-N and NO₂⁻-N removal rates of SBR2 in the same period. For both reactors, using average influent and effluent NH₄⁺-N, NO₂⁻-N, NO₃⁻-N, the stoichiometrically expected conductivity decreases from Anammox and denitrification (through both NO₂⁻-N and NO₃⁻-N routes) were calculated based on Table 1. The calculated conductivity decreases (around 90 μs/cm for SBR1, 205 μs/cm for SBR2) did not match with those observed (around 65 μs/cm for SBR1 (Figure 4(b)), 1,000 μs/cm for SBR2 (Figure 5(b))). Similarly to Phase I, SBR2 exhibited extremely high, about fivefold greater conductivity decreases with respect to the calculated values. This demonstrated that the use of mixed population seed makes process dynamics more complicated and eliminates the possibility of monitoring the start-up period by using real-time conductivity measurements.

In the third phase, the dominant process in the reactors was Anammox, hence NH₄⁺-N and NO₂⁻-N loadings to the reactors were gradually increased to enrich the Anammox culture (Figure 2). FISH analyses of sludge samples (images are not shown) proved the enrichment of Anammox species, mainly *Ca. Brocadia* and *Ca. Scalindua*, in both SBR1 and SBR2. The increasing acidity consumption rates expected in parallel to the increasing Anammox efficiencies were apparent in pH profiles as a gradually increasing pattern until the depletion of all NH₄⁺-N and NO₂⁻-N loaded to the systems (Figures 4(c) and 5(c)). The pH profiles

exhibited an 'apex' coinciding with the end point of NH₄⁺-N and NO₂⁻-N depletion. Following the end of Anammox, pH started to decrease gradually since the systems were continuously purged with an Ar/CO₂ gas mixture through the entire cycle time. The ceasing of CO₂ consumption with the end of Anammox resulted in solubilization of purged CO₂ in water and a pH drop. Similarly to Phase II, each cycle of reactors started with positive ORP due to NO₂⁻-N and NO₃⁻-N remaining in the reactors from the previous cycle. ORP slightly increased during the feeding stage. After feeding, ORP profiles exhibited a gradual decrease consistent with the ongoing NO₂⁻-N consumption due to Anammox. In both systems, ORP profiles reached a 'valley' which coincided with the end point of NO₂⁻-N and NH₄⁺-N removal. ORP gradually increased after the 'valley' with NO₃⁻-N production. Similarly to Phase I and Phase II, the conductivity profiles of both reactors exhibited a linear decreasing pattern with very high regression coefficients ($R^2 > 0.9$). The 'apex' point observed on pH profiles and the 'valley' point observed on ORP profiles exactly coincided with the end of the decrease in conductivity. No significant changes were observed in conductivity values after this point. For the observed NH₄⁺-N, NO₂⁻-N and NO₃⁻-N changes (Figures 4(c) and 5(c)), the conductivity decreases expected via Anammox through a batch cycle of SBR1 and SBR2 systems were calculated based on Table 1 as 1,584 and 1,541 μs/cm, respectively. These values roughly matched the observed conductivity decreases shown in Figures 4(c) and 5(c). The observed conductivity decreases through batch cycles of the enrichment phase were also evaluated for both systems against the observed total inorganic nitrogen (TIN) removal (Figure 6). The observed

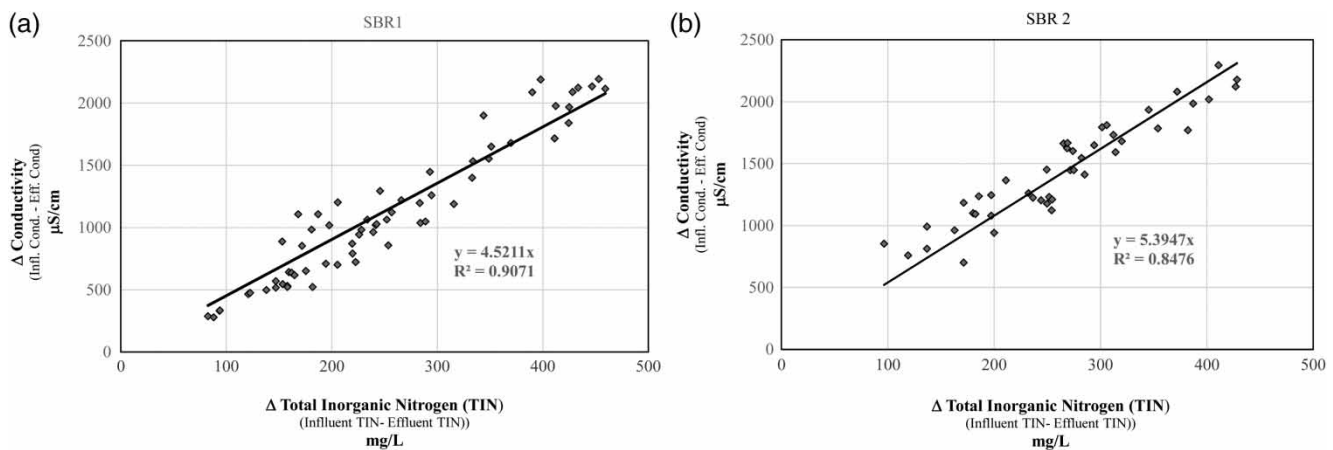


Figure 6 | Correlation between TIN removal and conductivity decreases observed through batch cycles of the enrichment phase (a) for SBR1 and (b) for SBR2.

conductivity decreases were well correlated with TIN removal for both SBR1 and SBR2. Despite markedly different inocula, close correlations obtained for both SBR1 and SBR2 encouraged the use of on-line conductivity monitoring for Anammox systems. The slopes of fitted lines in Figure 6 allow the predicting of expected TIN removal based on each unit conductivity ($\mu\text{S/cm}$) drop without a measurement of nitrogen species.

CONCLUSION

The overall findings demonstrated that the use of characteristic features of ORP and pH profiles without direct measurement of nitrogen species provides a quick and reliable monitoring of process dynamics in a newly started-up Anammox system. Independent of the origin of the seed culture, pH and ORP profiles provided distinctive trend lines including easily identifiable control points specific to endogenous denitrification and Anammox processes, which are the two major processes that usually continue simultaneously in newly started Anammox systems. Since these two simultaneously continuing processes cannot be clearly differentiated from each other via monitoring changes in nitrogen constituents only, utilization of pH and ORP profiles appear to be a powerful tool for providing insight into the biological state of a newly started-up Anammox system that other parameters may not reveal. A monitoring strategy to be developed based on real-time on-line pH and ORP measurements will make it possible to follow up nitrogen transformation process dynamics and to make necessary operational changes instantly, especially during the early start-up period of Anammox systems. This monitoring

strategy can be quite helpful for shortening the start-up period, which is the main challenge to a full-scale implementation of the Anammox process for wastewater treatment.

The quantitative correlation found between the observed conductivity decreases and changes in nitrogen species is quite valuable since a monitoring strategy based on conductivity measurements can effectively be used to adjust cycle time in SBR-type Anammox systems to achieve consistent effluent quality depending on fluctuations in influent wastewater strength.

ACKNOWLEDGEMENTS

The authors would like to thank TUBITAK (108Y120) for funding this study. The financial support of Marmara University (FEN-D-220513-0219) is also acknowledged. Special thanks to Elif Atasoy for her efforts to supply Anammox sludge from the Netherlands. Prof van Loosdrecht is acknowledged for supplying us with enriched Anammox seed. Istanbul Water and Sewerage Administration is acknowledged for allowing us taking sludge samples from Istanbul Pasakoy STP. Special thanks to Assoc. Prof. Alper Tunga Akarsubasi and his team for FISH analyses. Ercument Aktuz and Zehra Can are gratefully acknowledged for language editing.

REFERENCES

- Akın, B. S. & Ugurlu, A. 2005 [Monitoring and control of biological nutrient removal in a sequencing batch reactor](#). *Process Biochem.* **40**, 2873–2878.
- Bae, H., Park, K.-S., Chung, Y.-C. & Jung, J.-Y. 2010 [Distribution of anammox bacteria in domestic WWTPs and their enrichments](#)

- evaluated by real-time quantitative PCR. *Process Biochem.* **45**, 323–334.
- CRC 1999 *Handbook of Chemistry and Physics*, 80th edn, CRC Press, Boca Raton, FL, USA.
- Lackner, S. & Horn, H. 2012 Evaluating operation strategies and process stability of a single stage nitrification–Anammox SBR by use of the oxidation–reduction potential (ORP). *Bioresour. Technol.* **107**, 70–77.
- Li, H., Shaoqi, Z., Weihao, M., Guotao, H. & Bin, X. 2012 Fast start-up of ANAMMOX reactor: operational strategy and some characteristics as indicators of reactor performance. *Desalination* **286**, 436–441.
- Mulder, A., Van de Graaf, A. A., Robertson, L. A. & Kuenen, J. G. 1995 Anaerobic ammonium oxidation discovered in a denitrifying fluidized-bed reactor. *FEMS Microbiol. Ecol.* **16** (3), 177–183.
- Schmid, M. C., Maas, B., Dapena, A., van de Pas-Schoonen, K., van de Vossenberg, J., Kartal, B., van Niftrik, L., Schmidt, I., Cirpus, I., Kuenen, J. G., Wagner, M., Damste, J. S. S., Kuypers, M., Revsbech, N. P., Mendez, R., Jetten, M. S. M. & Strous, M. 2005 Biomarkers for in situ detection of anaerobic ammonium-oxidizing (Anammox) bacteria. *Appl. Environ. Microbiol.* **71** (4), 1677–1684.
- Standard Methods for the Examination of Water and Wastewater* 1998 20th edn. American Public Health Association/American Water Works Association/Water Environment Federation, Washington, DC, USA.
- Strous, M., Heijnen, J. J., Kuenen, J. G. & Jetten, M. S. M. 1998 The sequencing batch reactor as a powerful tool for the study of slowly growing anaerobic ammonium-oxidizing microorganisms. *Appl. Microbiol. Biotechnol.* **50**, 589–596.
- Sun, W., Banihani, Q., Sierra-Alvarez, R. & Field, J. A. 2011 Stoichiometric and molecular evidence for the enrichment of anaerobic ammonium oxidizing bacteria from wastewater treatment plant sludge samples. *Chemosphere* **84**, 1262–1269.
- Szatkowska, B., Plaza, E., Trela, J., Bosander, J. & Hultman, B. 2005 Application of conductivity measurements for monitoring of nitrogen removal in the partial nitrification/Anammox process. In: *Proceedings of the IWA Specialized Conference: Nutrient Management in Wastewater Treatment, Processes and Recycle Streams*, IWA Publishing, London, pp. 717–724.
- Van Der Star, W. R. L., Abma, W. R., Blommers, D., Mulder, J.-W., Tokutomi, T., Strous, M., Picioreanu, C. & van Loosdrecht, M. 2007 Startup of reactors for anoxic ammonium oxidation: experiences from the first full-scale Anammox reactor in Rotterdam. *Water Research* **41** (18), 4149–4163.
- Van Loosdrecht, M. & Salem, S. 2006 Biological treatment of sludge digester liquids. *Water Science and Technology* **53** (12), 11–20.

First received 6 December 2013; accepted in revised form 24 February 2014. Available online 15 March 2014